Available online at www.sciencedirect.com

ScienceDirect

Procedia IUTAM 21 (2017) 33 – 39

Procedia IUTAM

www.elsevier.com/locate/procedia

2016 IUTAM Symposium on Nanoscale Physical Mechanics

Nanocontact disorder in InP nanowire devices for the enhancement of visible light and oxygen gas sensitivities

Yen-Fu Lin[a], Chia-Hung Chang[a], Tsu-Chang Hung[a], Zhaoping Liu[b], Jiye Fang[b] and Wen-Bin Jian[a]*

[a]*Department of Electrophysics, National Chiao Tung University, Taiwan ROC*
[b]*Department of Chemistry, State University of New York at Binghamton, Binghamton, New York 13902-6000, USA*

Abstract

InP nanowires, synthesized through a self-seeded growth approach, are used in the fabrication of field-effect transistors which consist of source, drain, and back-gate electrodes. The weak gating voltage dependence implies low carrier concentrations whereas its behavior reveals native *n*-type doping in InP nanowires. These InP nanowire devices exhibit a vast variation of room-temperature resistance that raises a question about contact resistance. For devices of low room-temperature resistance, electron transport in InP nanowires is investigated using temperature dependent resistance in the temperature range between 80 and 300 K, and it can be analyzed using the model of thermal activation. For other devices of high room-temperature resistance, we take into account nanocontact resistance. Models of both Schottky contact and Mott's variable range hopping (VRH) are considered. The two resistances are connected in parallel to give total contact resistance of InP nanowire devices. After fitting experimental data by the proposed model, we estimate effective Schottky barriers and disorder contributions to nanocontact resistance. The effective Schottky barrier, and the nanocontact Schottky and Mott's VRH resistances are plotted as a function of the device room-temperature resistance which indicates the scale of disorder. Using room-temperature resistance of InP nanowire devices, the devices are classified into nanowire- or contact-dominated devices. The two different class of devices are used to check their photo- and gas-sensitivities. The contact-dominated InP nanowire devices show low dark current and low photocurrent as usual, but these contact-dominated devices give high ratio of photo- to dark-current. That result reveals a high photo-sensitivity for those devices of high nanocontact resistance. On the other hand, for gas sensing experiments, the contact-dominated devices show as well a high ratio of resistance under O_2 to that under N_2 gas exposure.

Peer-review under responsibility of organizing committee of Institute of the 2016 IUTAM Symposium on Nanoscale Physical Mechanics

* Corresponding author. Tel.: +886-3-571-2121ext56159; fax: +886-3-5725230.
E-mail address: wbjian@mail.nctu.edu.tw

Peer-review under responsibility of organizing committee of Institute of the 2016 IUTAM Symposium on Nanoscale Physical Mechanics
doi:10.1016/j.piutam.2017.03.034

Keywords: nanowire electronics; nanocontact; InP nanowire; disorder;

1. Introduction

The importance of the contact resistance in the investigation of intrinsic resistance of nanostructures has been pointed out when probing electron transport in nanomaterials such as carbon nanotubes.[1] In addition, the Schottky contact needs to be considered for the nanocontact formation between metal electrodes and semiconductor nanowires.[2] Moreover, the existence of disorder, presenting one-dimensional (1D) Mott's variable range hopping (VRH), in the contact between metal and semiconductor has been observed in Schottky diodes on *n*-type GaN.[3] The disorder effect in the nanocontact was observed in Pt contacts on GaN nanowire as well whereas the theory of two-dimensional (2D) Mott's VRH was implemented in analysis of experimental data.[4] On the other hand, the specific contact resistance of GaN nanowire devices has been studied and it was found to be dependent on the carrier density of the nanowire.[5] The importance of nanocontact resistance was then emphasized again and it was stressed that the small nanocontact area shall magnify the domination of specific contact resistivity. The magnified nanocontact resistance can dominate total resistance of nanowire devices.[6]

The III-V compound semiconductor InP has a direct band gap of 1.4 eV and it usually presents high sensitivity and photocurrent under visible light exposure.[7] Like ZnO, there are several kinds of defects, thus raising conductivity in InP.[7] InP played an essential role in optoelectronic integrated circuits[8] and, after integrated with InGaAs, InP heterojunction bipolar transistor revealed high operating speed.[9] On the other hand, InP was successfully converted to either *n*- or *p*-type nanowires by using laser assisted catalytic method.[10] Using both *n*- and *p*-type InP nanowires, nanoscale *p*-*n* junction was made and electroluminescence was measured from such a nanoscale light-emission diode.[10] Recently, another preparation method, the self-seeded growth, was developed to synthesize InP nanowires which were then used in the fabrication of field-effect transistors and Schottky devices.[11]

In this work, we will present investigation of intrinsic electrical properties of InP nanowire field-effect transistors. The dependence between the nanocontact resistance and the room-temperature (RT) resistance of nanowire devices is examined. The increase of disorder and nanocontact resistance give a high RT resistance for nanowire devices. The nanocontact resistance is then studied in devices having high RT resistance. After the temperature dependent resistance of nanocontact is analyzed, two types of nanocontact resistance are discovered. One type of nanocontact resistance originates from Schottky contact, coming from the contact between metal electrodes and InP nanowires. The other type of nanocontact resistance is due to nanoscale disorder that can be fitted by Mott's VRH. The InP nanowire devices are classified into either nanowire- or contact-dominated. The contact-dominated InP nanowire devices present a much high sensibilities when using as light or gas sensors.

2. Experimental Methods

The detail of the synthesis of InP nanowires, morphology of nanowires, and atomic structures have been described elsewhere.[12] The as-synthesized InP nanowires were kept in toluene. The InP nanowires were dispersed on the Si wafer substrate which was capped with a SiO_2 layer of 400-nm thick and was pre-patterned with micrometer-scale connection leads to large pads for measurements in a probe system. The substrate with InP nanowires dispersed was put in a high vacuum at 150ºC for 12 h to remove organic materials. A standard electron-beam lithography with thermal evaporation of Ti and Au (typically ~20 and ~100 nm in thickness) was used to deposit source and drain electrodes on InP nanowires. The Si substrate which is heavily *p*-type doped was used as a back-gate electrode. The morphology of nanowire devices is inspected using scanning electron microscope (SEM, JEOL JSM-7000F). The structure of the nanowire device is displayed in the inset to Fig. 1(a). The as-fabricated InP nanowire devices were put once more in a high vacuum at 400ºC for couple minutes to improve the electrical contact between metal electrodes and InP nanowires.

The as-fabricated nanowire devices were loaded in an insert cryostat (Dstat, CRYO Industries of America Inc.) and put in 1-atm helium gas. The electrometer (Keithley K6430) was used to obtain electrical features of current (I) as a function of voltage (V) at zero back-gate voltages ($V_G = 0$). The resistance was estimated at zero V_{BG} in a small source-drain voltage ranging from -10 to 10 mV. Other measurements, including transfer characteristics of field-effect transistors, photocurrent, and gas sensors, were done by placing InP nanowire devices in a high vacuum and all experiments were performed at RT. The photocurrent of InP nanowire devices was measured by shining a green light laser with a wavelength of ~532 nm and an intensity of 0.5 W/cm^2. The electrical signal due to gas exposure was measured when the chamber was put in the sequence of 1-atm oxygen gas, low vacuum, 1-atm nitrogen gas, and low vacuum again. It is suggested to read other published work[13,14] for a more detail description of our experimental methods.

3. Results and Discussions

Fig. 1(a) presents a SEM image of of InP nanowire devices from top view. The average diameter of the InP nanowire is about 21 nm. Two Ti/Au electrodes, deposited on top of nanowires, are regarded as source (S) and drain (D) electrodes. The substrate of a heavily p-type doped Si wafer is used as a back-gate (G) electrode at which a voltage V_G is applied to turn on/off the channel current in InP nanowires. The S, D, and G are basic electrodes of a typical field-effect transistor (FET) and the inset to Fig. 1(a) gives a complete structure of a nanowire FET device. The current (I) between S and D electrodes as a function of its voltage (V) at various temperatures is demonstrated in Fig. 1(b). The S-D current decreases more and more rapidly at a lower temperatures that indicates a semiconducting behavior of InP nanowires. To check the carrier type in the nanowire channel, the gating behaviors are shown in Figs. (c)-(f). Figs. (c) and (d) present the variation of S-D current (I) at three gating voltages. They show an increase of channel current at positive back-gate voltage which confirms n-type (electron) doping in InP nanowires. For a wider voltage range, as shown in Fig. 1(d), the current-voltage between S and D electrodes becomes nonlinear and asymmetric to that of the zero back-gate voltage. Figs. 1(e) and (f) provide gating behaviors at other back-gate voltages.

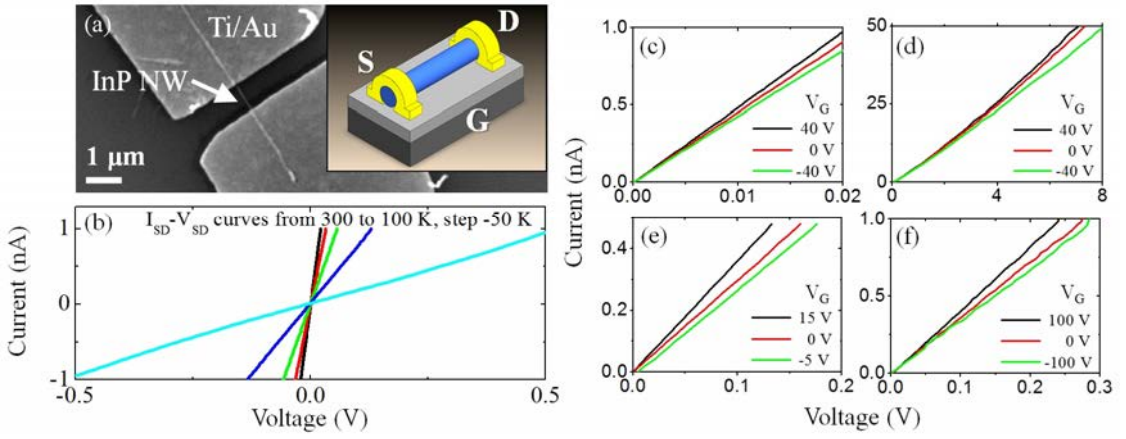

Fig. 1. (a) SEM image of a typical InP nanowire device where the Ti/Au electrodes are source (S) and drain (D) electrodes of a field-effect transistor. The substrate is used as a back-gate electrode (G) as indicated in the inset. (b) The *I-V* behavior of the InP nanowire device at different temperatures from 100 (light blue line) to 300 K (black line). The *I-V* behavior at different back gate voltages in a narrow and a wide S-D voltage range are displayed in Figs. (c) and (d), and those at other back-gate voltages are shown in Figs. (e) and (f).

A large amount of InP nanowire devices are fabricated and these devices usually exhibit different RT resistance and different temperature behaviors of resistance. As shown in Fig. 2(a), four typical InP nanowire FETs exhibit distinct temperature behaviors. Obviously, the four devices have different RT resistances and the highest RT resistance is about two orders of magnitude larger than the lowest RT resistance. For example, the RT resistance of the NW-A

device is ~5 GΩ and that of the NW-D device is ~90 MΩ. The diameter and crystallinity quality of InP nanowires shall be uniform thus such a big difference may originate from resistance in the nanocontact. As a consequence, we learn that the RT resistance is directly dependent on the nanocontact resistance of InP nanowire FET devices. At a temperature ranging from 80 to 300 K, the intrinsic electron transport and the resistance R as a function of temperature T in InP nanowires may simply be analyzed using thermal activation in the mathematical form of[13]

$$R_{\mathrm{TH}}(T) = R_{\mathrm{TH},0}\exp(E_{\mathrm{a}}/k_{\mathrm{B}}T), \tag{1}$$

where $R_{\mathrm{TH},0}$ is a constant, k_{B} is Boltzmann constant, and E_{a} is activation energy for carriers in InP nanowires. The solid lines in Fig. 2(a) delineate fitting to experimental data for devices having different RT resistances. It is obvious that resistance of devices with high RT resistance is described by Eq. (1) only in a very short temperature range at high temperatures. At low temperatures, the resistance of high RT resistance devices may be dominated by nanocontact resistance which will be discussed later. To investigate more about intrinsic electrical properties of InP nanowires, we measured the resistance of the device with the lowest RT resistance and analyzed the temperature behavior of resistance. Fig. 2(b) presents the best fitting to our experimental data. Because the intrinsic resistance of InP nanowires is in a wide temperature range down to 10 K, an additional theory of three-dimensional (3D) Mott's VRH has to be introduced. The 3D Mott's VRH is of expressed as the form of[15]

$$R_{\mathrm{VRH}}(T) = R_{\mathrm{VRH},0}\exp\left((T_0/T)^{1/(1+d)}\right), \tag{2}$$

where $R_{\mathrm{VRH},0}$ is a constant, T_0 is a parameter about the strength of disorder, and the dimension of the electron system $d = 3$ is used for InP nanowires. Since the two conduction mechanisms are connected in parallel, the total resistance of InP nanowire is fitted by using the function of $R_{\mathrm{NW}}(T)$, where $\mathrm{R}_{\mathrm{NW}}^{-1} = R_{\mathrm{TH}}^{-1} + R_{\mathrm{VRH}}^{-1}$. Fig. 2(b) presents the best fitting. The resistance at temperatures lower than 60 K is dominated by 3D Mott's VRH whereas that at high temperatures is described very well by thermal activation.

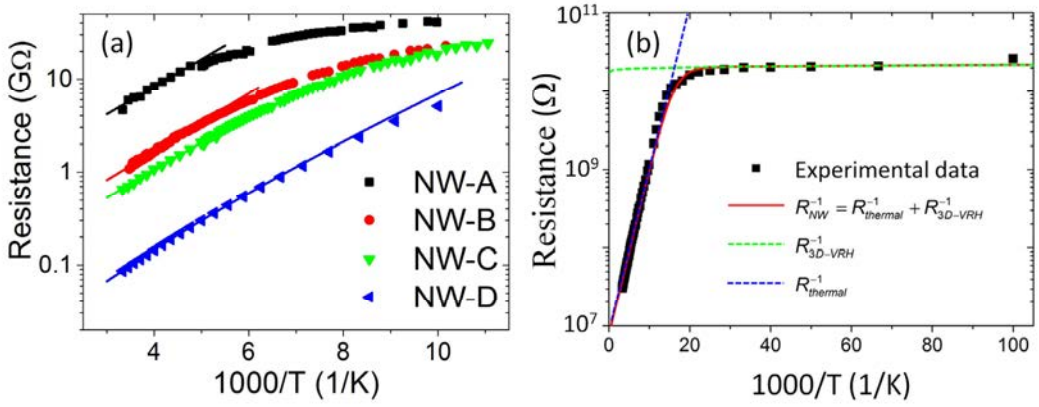

Fig. 2. (a) Resistance as a function of inverse temperature for InP nanowire devices of various RT resistances. The temperatures are in the range between 100 and 300 K. The RT resistances of NW-A to NW-D devices are about 5 GΩ, 1 GΩ, 650 MΩ, and 90 MΩ. The lines are the best fittings according to the theoretical model of thermal activation. (b) Resistance varied in a wide temperature range between 10 and 300 K for the InP nanowire device having RT resistance of ~30 MΩ. The intrinsic resistance of InP nanowire is fitted by theoretical models of both thermal activation and 3D Mott's VRH (red line). The blue and green dashed lines show the contribution of device resistance from thermal activation and 3D Mott's VRH, respectively.

The intrinsic electron transport in InP nanowires is reasonably explained. Then, we want to look into the nanocontact resistance of nanowire FET devices with high RT resistance. As presented in the introduction section, two mechanisms need to be considered for the nanocontact resistance. One is the Schottky contact resistance due to a metal-to-semiconductor contact and the other is disorder in nanocontact. Furthermore, it is argued in the literatures

that disorder in contact shows either 1D or 2D Mott's VRH and, in our previous report,[6] disorder in nanocontact shows a variation from 1D to 3D Mott's VRH. Thus, we do not freeze the dimensional parameter d of Eq. (2) in the following fitting work. Fig. 3(a) presents a systematic temperature behaviors for nanowire devices of different RT resistances in the temperature range from 80 to 300 K. The inset gives a simple circuit model that we used to analyze our data. In this temperature range, thermal activation (Eq. (1)) is used to describe the intrinsic resistance of InP nanowires whereas two mechanisms, Schottky contact and Mott's VRH, are used to express a temperature behavior of nanocontact resistance. The Schottky contact resistance is presented in the form[16]

$$R_{\mathrm{SC}} = \left(R_{\mathrm{SC},0}/T\right)\exp(q\Phi_{\mathrm{BE}}/k_{\mathrm{B}}T), \tag{3}$$

where $R_{\mathrm{SC},0}$ is a constant, q is the charge of carriers, and Φ_{BE} is the effective Schottky barrier height. The two mechanisms of nanocontact resistance contribute in parallel thus the total contact resistance $R_{\mathrm{NC}}(T)$ is given by $R_{\mathrm{NC}}^{-1} = R_{\mathrm{SC}}^{-1} + R_{\mathrm{VRH}}^{-1}$. The total device resistance including the contact and the nanowire resistances is fitted by $R_{\mathrm{TH}} + R_{\mathrm{NC}}$, where the resistance of thermal activation (R_{TH}) is used to describe intrinsic temperature behaviors of nanowires. The curves of data fitting according to the model are plotted in Fig. 3(a) as well.

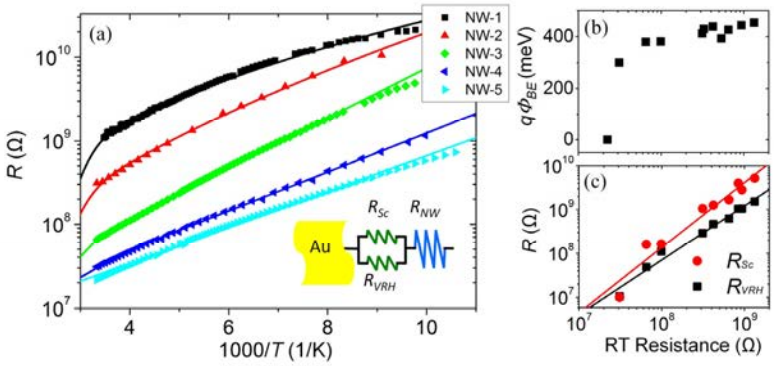

Fig. 3. (a) Resistance as a function of inverse temperature for InP nanowire devices (NW1-NW5) at temperatures ranging from 80 to 300 K. The RT resistance of the NW1 to NW5 devices are about 1 GΩ, 310 MΩ, 65 MΩ, 30 MΩ, and 22 MΩ.The inset shows the equivalent circuit, including the Schottky contact, the disordered contact (Mott's VRH), and the intrinsic nanowire resistance (thermal activation), used for data analyses. (b) The effective Schottky barrier height $q\Phi_{\mathrm{BE}}$ as a function of RT resistance of InP nanowire devices. (c) Resistance from the Schottky and the Mott's VRH as a function of RT resistance of InP nanowire devices. The solid lines are guide to eyes.

The extracted parameter of the effective Schottky barrier $q\Phi_{\mathrm{BE}}$ is drawn as a function of RT resistance and presented in Fig. 3(b). It is surprisingly that the $q\Phi_{\mathrm{BE}}$ is systematically dependent on RT resistance of InP nanowire devices. This systematic dependency confirms correct physical mechanisms used in our model for data analysis. With a small increase of RT resistance, the $q\Phi_{\mathrm{BE}}$ starts from zero and increases rapidly to a saturated value of about 400 meV. It is interestingly that, on devices having the lowest contact resistance, Ti metal film does not produce any Schottky contacts on InP nanowires. The Schottky contact suddenly appears when the nanocontact resistance is higher and starting to contribute to total device resistance. As pointed out previously, the two resistances of Schottky contact and Mott's VRH are connected in parallel. We plot the two contact resistance as a function of RT resistance in Fig. 3(c). For a parallel connection of circuit, the lower the resistance is, the higher in ratio it will dominate to the total resistance. Mott's VRH dominates to the total nanocontact resistance for InP nanowire devices having high RT resistances. The systematic variation of resistance owing to the two different mechanisms corroborates, again, the correctness of our model and our data analysis.

According to previous results, we rationally suggest that the control of Ti film deposition is essential in determination of disorder in nanocontat. For a direct contact of pure Ti film on InP nanowires, the nanocontact resistance is much smaller than the nanowire resistance. On the other hand, when the Ti film deposition is not in high

vacuum, some residue O_2 gas will be introduced. Thus the control of background vacuum pressure will possibly help to control the disorder in nanocontact. We have reproduced making high RT resistance devices by thermal evaporation of Ti metal film in a vacuum level of 10^{-5} torr.

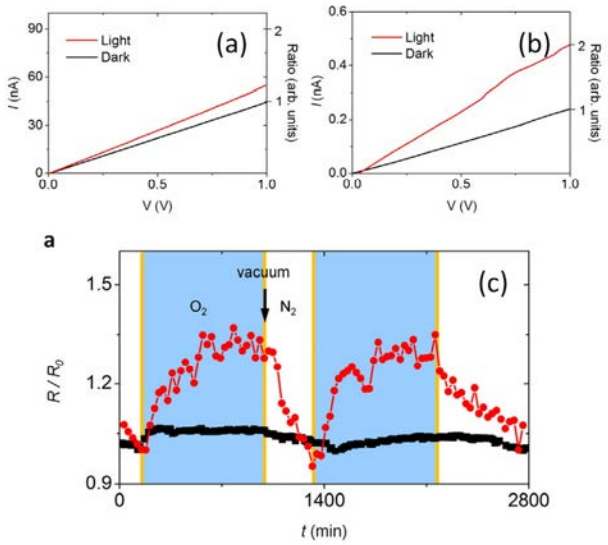

Fig. 4. (a) Current-voltage (*I*-*V*) behavior of a typical nanowire-dominated device (RT resistance of ~22 MΩ) with and without exposing to green light. (b) Current-voltage behavior of a typical contact-dominated device (RT resistance of ~4 GΩ) with and without exposing to green light. (c) Ratio of resistance variation of nanowire-dominated (black squares, RT resistance of ~30 MΩ) and the contact-dominated (red circles, RT resistance of ~690 MΩ) devices in response to exposure of O_2 gas. After the O_2 exposure, the device is put in low vacuum and then it is exposed to N_2 gas.

It is clear that the increase of RT resistance of InP nanowire devices are mainly due to introduced disorder in nanocontact. We may then classified InP nanowire devices as contact- and nanowire-dominated devices for devices having high and low RT resistance, respectively. In the next step, we look into special nanocontact properties and find out any possible applications. We employ the contact- and nanowire-dominated InP nanowire devices to be light and gas sensors. Figs 4(a) and 4(b) present green light sensitivities of nanowire- and contact-dominated InP devices. The left *y*-coordinate gives the absolute current whereas the right *y*-coordinate gives the ratio between photocurrent and the dark current at $V = 1$ V. The absolute values show that photocurrent in nanowire-dominated devices is two orders of magnitude higher than that in contact-dominated devices. This is rational because a disorder in nanocontact will cause a serious reduction of dark- and photo-current. The ratio of the photo- to dark-current of nanowire-dominated devices is, nevertheless, much lower than that of contact-dominated devices. Thus, the nanocontact disorder raises the light sensitivities of InP nanowire devices.

In addition, the gas sensitivities of nanowire- and contact-dominated devices are measured and expressed in Fig. 4(c). The variation of resistance is expressed as the ratio of the resistance under gas exposure to the device RT resistance. The variation ratio of nanowire-dominated devices is obviously lower in response to O_2 gas exposure when comparing with contact-dominated devices. As a consequence, the nanocontact disorder raises the O_2 gas sensitivities of InP nanowire devices evidently.

4. Conclusion

InP nanowire FET devices have been made. According to transfer characteristics of InP nanowire FET devices, the channel material of InP nanowires exhibits natively *n*-type doping. After inspecting RT resistance of a large amount of InP nanowire devices, we discover the domination of nanocontact resistance for devices having high RT resistance.

For the device of the lowest RT resistance, the device resistance is dominated by intrinsic InP nanowire resistance. Its temperature behavior shows thermal activation and 3D Mott's VRH at temperatures above and below ~60 K, respectively. For nanowire devices having high RT resistance, we analyzed resistance at temperatures ranging from 80 to 300 K by thermal activation, Schottky contact, and Mott's VRH. Here the Mott's VRH could be a 1D, 2D or 3D system for disorders in nanocontact. The fitting results give the effective Schottky barrier height in nanocontact. More interestingly, the Schorrky barrier height is rationally dependent on RT resistance of devices where the RT resistance is taken as a scale of disorder. The InP nanowire devices are then classified into contact- and nanowire-dominated devices according to their RT resistances. We investigate the application of nanocontact disorder in sensors including light and gas sensibilities. We discover that the nanocontact disorder gives rise to a very high sensitivities in optical and gas sensing.

Acknowledgements

This work was supported by the Taiwan National Science Council under Grant Numbers MOST 103-2628-M-009-004-MY3 and MOST 104-2119-M-009-009-MY3, and by the MOE ATU Program.

References

1. Dai H, Wong EW, Lieber CM. Probing electrical transport in nanomaterials: conductivity of individual carbon nanotubes. *Science* 1996;**272**:523-526.
2. Landman U, Barnett RN, Scherbakov AG, Avouris P. Metal-semiconductor nanocontacts: silicon nanowires. *Phys. Rev. Lett.* 2000;**85**:1958-1961.
3. Miller EJ, Yu ET, Waltereit P, Speck JS. Analysis of reverse-bias leakage current mechanism in GaN grown by molecular-beam epitaxy. *Appl. Phys. Lett.* 2004;**84**:535-537.
4. Nam CY, Tham D, Fischer JE. Disorder effects in focused-ion-beam-deposited Pt contacts on GaN nanowires. *Nano Lett.* 2005;**5**:2029-2033.
5. Stern E, Cheng G, Young MP, Reed MA. Specific contact resistivity of nanowire devices. *Appl. Phys. Lett.* 2006;**88**:053106.
6. Lin YF, Jian WB. The impact of nanocontact on nanowire based nanoelectronics. *Nano Lett.* 2008;**8**:3146-3150.
7. Jansen RW. Theoretical study of native defects and impurities in InP. *Phys. Rev. B* 1990;**41**:7666-7673.
8. Müller G. InP – the basic material of integrated optoelectronics for fiber communication systems. Phys. Scr. 1991;T35:201-209.
9. Chandrasekhar S. Optoelectronic system integration using InP-based HBTS for lightwave communications. *Solid-State Electron.* 1997;**41**:1413-1417.
10. Duang X, Huang Y, Cui Y, Wang J, Lieber CM. Indium phosphide nanowires as building blocks for nanoscale electronic and optoelectronic devices. *Nature* 2001;**409**:66-69.
11. Strupeit T, Klinke C, Kornowski A, Weller H. Synthesis of InP nanoneedles and their use as Schottky devices. *ACS Nano* 2009;**3**:668-672.
12. Liu Z, Sun K, Jian WB, Xu D, Lin YF, Fang JY. Soluble InP and GaP nanowires: self-seeded, solution-liquid-solid synthesis and electrical properties. *Chem. Eur. J.* 2009;**15**:4546-4552.
13. Lin YF, Chen TH, Chang CH, Chang YW, Chiu YC, Hung HC, Kai JJ, Liu Z, Fang J, Jian WB. Electron transport in high-resistance through two-probe measurements. *Phys. Chem. Chem. Phys.* 2010;**12**:10928-10932.
14. Lin YF, Chang CH, Hung TC, Jian WB, Tsukagoshi K, Wu YH, Chang L, Liu Z, Fang J. Nanocontact disorder in nanoelectronics for modulation of light and gas sensitivities. *Sci. Rep.* 2015;**5**:13035.
15. Mott NF. Conduction in non-crystalline materials (Oxford Univrsity Press (UK) 1993).
16. Sze SM, Ng KK. Physics of semiconductor devices (John Wiley & Sons, 2006) third edn